HHS Public Access

Author manuscript

Sci Total Environ. Author manuscript; available in PMC 2020 June 01.

Published in final edited form as:

Sci Total Environ. 2019 February 01; 649: 1189–1197. doi:10.1016/j.scitotenv.2018.08.360.

Effectiveness of zinc oxide-assisted photocatalysis for concerned constituents in reclaimed wastewater: 1,4-Dioxane, trihalomethanes, antibiotics, antibiotic resistant bacteria (ARB), and antibiotic resistance genes (ARGs)

Myung Hwangbo[a], **Everett Caleb Claycomb**[b], **Yina Liu**[c], **Theodore E.G. Alivio**[d,e], **Sarbajit Banerjee**[d,e], **Kung-Hui Chu**[a,*]

[a]Zachry Department of Civil Engineering, Texas A&M University, College Station, TX 77843-3136, USA

[b]Department of Petroleum Engineering, Texas A&M University, College Station, TX 77843-3116, USA

[c]Geochemical and Environmental Research Group, Texas A&M University, College Station, TX 77843-3136, USA

[d]Department of Chemistry, Texas A&M University, College Station, TX 77843-3012, USA

[e]Department of Materials Science and Engineering, Texas A&M University, College Station, TX 77843-3003, USA

Abstract

Microbial and emerging chemical contaminants are unwanted constituents in reclaimed wastewater, due to the health concerns of using the water for agricultural irrigation, aquifer recharges, and potable water. Removal of these contaminants is required but it is currently challenging, given that there is no simple treatment technology to effectively remove the mixture of these contaminants. This study examined the effectiveness of ZnO-assisted photocatalytic degradation of several constituents, including 1,4-dioxane, trihalomethanes (THMs), triclosan (TCS), triclocarban (TCC), antibiotic resistant bacteria (ARB) and antibiotic resistant genes (ARGs), under low intensity of UV exposure. *E. coli* with an ARGs-carrying circular plasmid (pUC19) was used as a model antibiotic resistant bacterium. Our results show that commercial zinc oxide (C-ZnO) assisted photodegradation of 1,4-dioxane, and dehalogenation of THMs, TCS, and TCC, while tetrapodal zinc oxide (T-ZnO) enhanced the dehalogenation of TCS and TCC. Additionally, T-ZnO assisted the photocatalytic inactivation of the *E. coli* within 6 h and caused structural changes in the plasmid DNA (pUC19) with additional UV exposure, resulting in nonfunctional AGR-containing plasmids. These results also suggest that higher UV dose is required not only to inactivate ARB but also to damage ARGs in the ARB in order to decrease risks in promoting ARB population in the environment. Overall, our results implicated that, under

*Corresponding author at: 402A DLEB, Civil Engineering Department, Texas A&M University, 3136 TAMU, College Station, TX 77843-3136, USA. kchu@civil.tamu.edu (K.-H. Chu).

Appendix A. Supplementary data

Supplementary data to this article can be found online at https://doi.org/10.1016/j.scitotenv.2018.08.360.

low UV intensity, ZnO-assisted photocatalysis is a promising alternative to simultaneously remove biological and emerging chemical contaminants in treated wastewater for safe reuse.

GRAPHICAL ABSTRACT

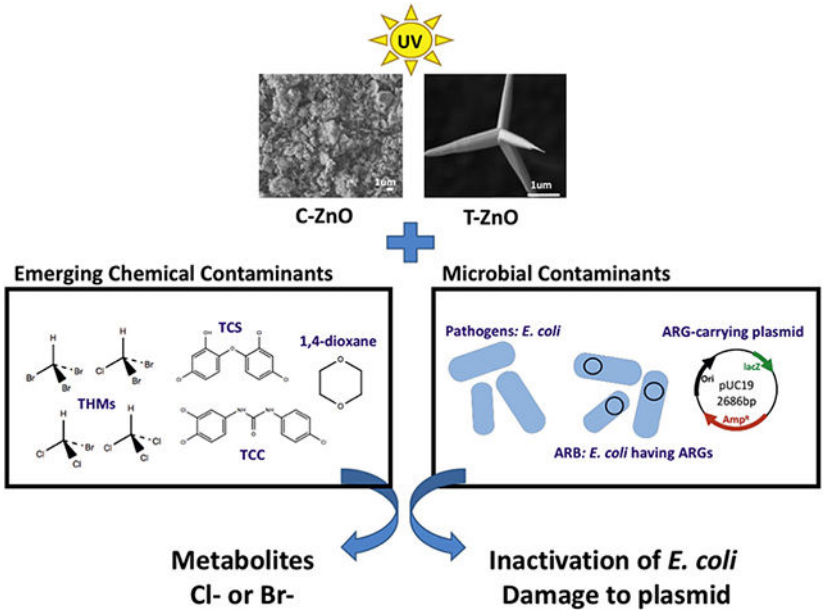

C-ZnO = commercial zinc oxide; T-ZnO = tetrapod zinc oxide; ARB = antibiotic resistant bacteria; ARGs = antibiotic resistant genes.

Keywords

Emerging contaminants; Reclaimed water; Photocatalytic degradation; Zinc oxide; Bactericidal effects; Plasmid DNA breaking

1. Introduction

Beneficial uses of treated wastewater (referred as reclaimed water) can be a viable strategy to supplement increasingly limited fresh water resources to meet the freshwater demand of the growing human population (State Water Resources Control Board, 2018). Treated wastewater from conventional wastewater treatment processes, however, often contains biological contaminants and traces of emerging chemical pollutants. The presence of these constituents in treated wastewater not only raises concern in human health but also decreases public acceptance of the reuse. To address these issues in reclaimed water, effective treatment methods for removing these contaminants are required.

Reclaimed water contains many contaminants, including disinfection byproducts (DBPs), antimicrobial agents, and 1,4-dioxane (Du et al., 2017; Estevez et al., 2012; Lv et al., 2017; Richardson and Kimura, 2017). According to the 2012 U.S. Environmental Protection Agency (USEPA) Guidelines for Water Reuse, antimicrobial agents, DBPs, and 1,4-dioxane should be removed for water reuse (USEPA, 2012). DBPs like trihalomethanes (THMs) are

known carcinogens and potential mutagens. Due to their toxicity to humans and other organisms, the USEPA has set a maximum contaminant level of 0.080 mg/L for total THMs in drinking water in 2013. Triclosan (TCS) and triclocarban (TCC) are widely used antimicrobial agents in various personal care products, hospitals, and industries. Moreover, TCS and TCC are endocrine-disrupting compounds (Gee et al., 2008; Lee et al., 2012) and are commonly detected in treated wastewater at ng/L to μg/L levels (Healy et al., 2017; Lee et al., 2012; McMurry et al., 1998). Both TCC and TCS can potentially convert to more toxic chlorinated compounds in the environment (Halden et al., 2017). For example, upon UV exposure, TCS may be degraded into two different dioxins (2,7-dibenzodichloro-p-dioxin and 2,8-dibenzodichloro-p-dioxin) (Buth et al., 2010; Lee et al., 2012; Rule et al., 2005). TCS can be degraded to harmless endproducts by pure cultures (Lee et al., 2012; Lee and Chu, 2013). TCC may be transformed into chlorinated anilines, which are compounds of concern due to their toxicity (Halden and Paull, 2005). In 2016, the U.S. Food and Drug Administration (FDA) banned the use of TCS and TCC in personal care products such as hand and body washes. Yet, these two compounds are still used in hospitals and food service settings (FDA, 2016). While 1,4-Dioxane is biodegradable (Hand et al., 2015), it has been detected in treated wastewater. As 1,4-dixoane is a suspected carcinogen, US EPA has issued a lifetime health advisory of 0.2 mg/L and a screening level of 0.67 μg/L for 1,4-dioxane (USEPA, 2017).

In addition to pathogens, antibiotic resistant bacteria (ARB) and antibiotic resistant genes (ARGs) are also microbial contaminants in reclaimed water. These biological contaminants pose potential risks in spreading foodborne diseases when reclaimed water was used for agricultural irrigation (Kim et al., 2013; Rosario et al., 2009; Rose, 2007). ARB and ARGs can spread easily into non-ARB through horizontal gene transfer, transposons, and integrons, and thus pose risks in promoting ARB population (Hong et al., 2013; Pruden et al., 2013; Wang et al., 2014). Therefore, an effective treatment process that can remove all of these contaminants in reclaimed water is necessary to mitigate the potential public health risks and to increase public acceptance of reclaimed water.

Advanced oxidation process based on photocatalysis has shown a potential for removing chemical and microbial contaminants (Kim et al., 2013; Lee et al., 2016; Schneider et al., 2014). Previous studies using titanium dioxide (TiO_2) as photocatalyst with strong UV exposure have shown to degrade pesticides (365 nm, 350 W) (Zhu et al., 2005), TCS (365 nm, 15 W) (Yu et al., 2006), TCC (265 nm, 300 W) (Ding et al., 2013), 1,4-dioxane (10–400 nm, 100 W) (Alvarez-Corena et al., 2016), and to inhibit microbial growth by damaging cell membrane or breaking DNA strands (Kim et al., 2013; Liu and Yang, 2003; Sirelkhatim et al., 2015). Compared to TiO_2, zinc oxide (ZnO) is an attractive alternative photocatalyst because ZnO is more economical and can be excited by a broad UV spectrum, ranging from 245 nm to 380 nm (Akhmal Saadon et al., 2016). Under UV irradiation (365 nm, 100 W), ZnO plates (50 mm × 60 mm) photodegraded synthetic dyes such as methylene blue (Akhmal Saadon et al., 2016). Photodegradation of humic acid by commercial ZnO nanoparticle under mercury lamp (125 W) (Oskoei et al., 2016) and phenolic compounds by ZnO/nanoclinoptilolite powders under Hg lamp (75 W) (Nezamzadeh-Ejhieh and Khodabakhshi-Chermahini, 2014) have been reported.

Interestingly, while no photodegradation of 5:3 polyfluorinated acid (5:3 acid) was not observed in the presence of commercial TiO_2, high removal of 5:3 acid (96%) was observed in the presence of tetrapodal ZnO (hereafter referred as T-ZnO) (Abada, 2016). Furthermore, we recently observed a better dechlorination of TCS by T-ZnO (75% dechlorinated) than by commercial TiO_2 (50% dechlorination) under UV exposure (data not shown). However, whether ZnO excited under long-UV wavelengths can photodegrade biological and emerging chemical contaminants in the reclaimed water is largely unknown. Photocatalysis of THMs using TiO_2 or ZnO has not been reported by previous studies. Furthermore, it is unclear whether photocatalysis can damage the ARGs in the ARB, or the ARGs released from inactivated ARB into the environment can be incorporated by other microorganisms that originally do not processes with ARGs.

This study focused on the potential use of ZnO as a photocatalyst to remove chemical and microbial contaminants in reclaimed water. Specifically, we focus on identifying optimal conditions to inactivate pathogens, to damage the ARGs in ARBs, and to degrade emerging chemical contaminants. Additionally, experiments were designed to examine the uptake potential of free, ARG-carrying plasmids by other microorganisms. *E. coli* containing an ARG-carrying plasmid and ARG-carrying plasmids were used as model microbial contaminants. Three different types of emerging chemical contaminants, DBPs (THMs and chloroform), 1,4-dioxane, antibiotics (TCS and TCC) were used as model contaminants. The degradation potential of these model contaminants was determined in the presence and/or absence of ZnO at long wavelength (365 nm) under low UV intensity (4 W/m^2) conditions. Reusability of ZnO for TCS and TCC removal was also determined.

2. Material and methods

2.1. Chemicals

Triclosan (5-chloro-2-(2,4-dichlorophenoxy)-phenol, TCS, 97% pure), triclocarban (3-(4-chlorophenyl)-1-(3,4-dichlorophenyl) urea, TCC, 99% pure), chloroform (99.5% pure), dichloromethane (99.8% pure), ethyl acetate (99.9% pure), and Commercial ZnO (hereafter referred as C-ZnO) (99% pure) were purchased from Sigma-Aldrich Co. (St. Louis, MO). 1,4-Dioxane (99% pure) was purchased from Alfa-Aesar (Haverhill, MA). Trihalomethane mixture (THMs) including bromodichloromethane, bromoform, chloroform, and dibromochloromethane (200 μg/mL each), was purchased from Fisher Scientific (Pittsburgh, PA). *N,O*-bis(trimethylsilyl)-trifluoroacetamide (BSTFA) with 1% trimethylchlorosilane (TMCS) were purchased from Pierce Biotechnology Inc. (Rockford, IL). Deionized water (DI water) was produced from a Milli-Q system. Stock solutions of TCS and TCC (1 g/L) were prepared in acetone. TZnO were synthesized from Zn metal (99%, McMaster-Carr, Elmhurst, IL) as described previously (O'Loughlin et al., 2017). T-ZnO has an average of 12 m^{-1} surface area to volume ratio (O'Loughlin et al., 2017). Table S1 in SI lists the characteristics of T-ZnO and CZnO and their scanning electron microscope (SEM) images.

2.2. Photocatalytic degradation of emerging chemical contaminant

Photocatalytic degradation tests were conducted in a series of glass vials. Each vial contained one of the model chemical contaminants in the presence or absence of two

different types of ZnO (C- or T-ZnO). Briefly, a series of 20-mL glass vials containing 5 mL DI water with or without ZnO (1 g/L) were sealed with Teflon-coated septa and screw caps. Each vial was spiked with a known amount of each of the model chemical contaminants to achieve an initial concentration of 20 mg/L for 1,4-dioxane (Hand et al., 2015), or 3 mg/L for THMs and chloroform. Acetone-free TCS and TCC solution was used for TCS or TCC photodegradation tests. Acetone-free TCS and TCC solutions were prepared by adding a known amount of TCS or TCC stock solution into an empty 100-mL glass vial. After acetone was evaporated, a known amount of DI water was then added into the vial with overnight shaking to reconstitute TCS or TCC in DI water (Lee et al., 2012). The water solubility of TCS is 12 mg/L (USEPA, 2008) and TCC is 0.11 mg/L (as determined in the laboratory) at 20 °C. The initial concentrations of 5 mg/L for TCS and 0.11 mg/L for TCC were used for photocatalytic experiments. After shaking overnight, C-ZnO or T-ZnO (1 g/L) was added into the vial and stirred with a magnetic stir bar for 30 min in the dark to allow adsorption of the contaminants on to the surface of ZnO. Subsequently, a 5 mL aliquot of the mixture were collected into a 20-mL vial. Photodegradation was initiated by exposure of the vials to UV light (4 W, 365 nm) with constant shaking at 250 rpm for 2 days. Time-course degradation experiments for 1,4-dioxane, TCS, and TCC were also conducted. Triplicate samples were used in each set of degradation experiments. Two different types of controls, one containing ZnO and contaminant without UV exposure and the other one containing the contaminant with only UV exposure, were used. Reusability of T-ZnO was also determined and a detailed description is available in SI.

2.3. Chemical analysis

Concentrations of 1,4-dioxane were analyzed by Agilent 6890N Gas Chromatography (GC, Agilent 6890N)/Flame Ionization Detection (FID) equipped with a J&W 122–5532G capillary column as described by Hand et al. (Draper et al., 2000; Hand et al., 2015). Concentrations of TCS were analyzed using a GC/Mass Spectrometer (MS, Agilent 5973) equipped with DB-5 column as described previously (Lee et al., 2012; Roh et al., 2009). Concentrations of TCC were determined by a High-Performance Liquid Chromatography (HPLC, Agilent 1290 Infinity II)/Triple Quadrupole Mass Spectrometer (QqQ-MS, Agilent 6470) equipped with a Jet Stream electrospray ionization source. Chloride ions and bromide ions were measured by an Ion Chromatography (Dionex Integrion HPIC, Thermo Fisher) system equipped with an IonPac AS19–4 μm analytical column (4 × 250 mm). All detailed description of chemical analysis is available in SI.

2.4. Photocatalytic inactivation of pathogen and ARB and degradation of ARG-carrying plasmid

Experiments were designed to evaluate three specific scenarios: (i) inactivation of pathogens, (ii) damage of ARGs in ARB, and (iii) potential uptake of ARGs by other microorganisms. The ARGs might be present in reclaimed water resulting from the decay of ARB. In this study, *E. coli* (NEB5-alpha) was used as a surrogate for pathogens. To create an ARB, a plasmid pUC19 containing ampicillin resistant genes (Amp^R) was transformed into *E. coli* cells (NEB5-alpha) chemically. The *E. coli* carrying pUC19 (referred as *E. coli*-pUC19 hereafter) was used to represent an ARB.

Photocatalytic inactivation experiments using *E. coli*-pUC19 were likewise conducted. Viable *E. coli* in the supernatant was determined using plate counting. Details of the experiment and plate counting are described in SI. Gel electrophoresis was conducted for plasmids extracted from supernatants of treated samples to determine the structural change or damage (detailed description in SI). Photocatalytic experiments using plasmid DNA pUC19 were conducted similarly as described for photocatalytic inactivation of *E. coli*-pUC19 experiments, except plasmid pUC19 was used. This experiment was conducted to determine if plasmid DNA pUC19 can be structurally changed or damaged by photocatalysis using ZnO (detailed description in SI).

3. Results

3.1. Photocatalysis of THMs, chloroform, 1,4-dioxane under low UV irradiation

Experiments were conducted to determine if trace chemicals such as THMs, chloroform, and 1,4-dioxane can be removed by C-ZnO under low UV irradiation. The mixture of THMs used in this study contains four different compounds: bromoform, dibromochloromethane, bromodichloromethane, and chloroform. Mineralization of these halogenated chemicals was expected to release free chloride and bromide ions, which can be used to quantify the effectiveness of removal of these compounds. Fig. 1a-i and a-ii show photocatalysis of THMs, with 22% dechlorination and > 100% debromination. Under the same conditions, C-ZnO caused approximately 90% dechlorination of chloroform (no other compounds present) (Fig. 1a-iii). The results suggested that brominated THMs are degraded more readily than chlorinated THMs via photocatalysis, which may be due to weaker chemical bond strength of C–Br than that of C–Cl, given the theoretical bond energy for C–Br is 285 kJ/mol and for C–Cl is 327 kJ/mol (Gilday et al., 2015).

Complete photocatalytic degradation of 1,4-dioxane by C-ZnO within 12 h was observed, while UV alone can also degrade 30% of 1,4-dixoane (Fig. 1b) within the same timeframe. The first-order degradation rate constant (k) for 1,4-dioxane was estimated to be0.456 min^{-1} based on data taken before 12 h (Table 1). Together, CZnO has showed a potential to photocatalyze these emerging contaminants within 24 h in the presence of C-ZnO under low UV intensity.

3.2. Degradation of antimicrobial agents, TCS and TCC, under low UV irradiation

Both C-ZnO and T-ZnO can photodegrade TCS and TCC after 24 h of UV exposure, based on dechlorination efficiency (defined by the amounts of halide anions released over the theoretical halogens of the amount of contaminant degraded) (Fig. S1 in SI). In the absence of ZnO, regardless types of ZnO, only a small amount of chloride was released (<3.5%), suggesting that the intensity of UV exposure used in this study might not be sufficient to dechlorinate TCS and TCC. However, under the same UV exposure, dechlorination of TCS and TCC was enhanced in the presence of photocatalysts ZnO. A better contaminant degradation performance was expected for T-ZnO than for C-ZnO, based on their defined morphology and large surface area to volume ratio (Table S1 in SI). However, as shown in Fig. S1, this expectation was only true for TCS dechlorination (75% TCS dechlorination with T-ZnO vs 59% TCS dechlorination with C-ZnO). Complete TCC dechlorination

efficiency (i.e., all halide anions were released from the amount of TCC degraded) was observed for T-ZnO and C-ZnO. The high dechlorination for TCC might be contributed by several factors including low amount of TCC degraded, differences in chemical structures and properties between TCS and TCC, and UV energy needed for dechlorinating different photolysis products of TCS and TCC. There are structural differences between TCC and TCS. TCS has an ether bond linking two chlorinated phenyl rings, while TCC also has two chlorinated phenyl rings, TCC has two additional N–H bonds in the structure and is more similar to diphenylcarbamide. The difference is thus led to different photolysis products of TCC and those of TCS which have been previously observed. For example, TiO_2-assisted photodegradation of TCC generated photolysis products such as 3,4-dichloroaniline, 4-chloroaniline, 4-chloroisocyanatobenzene, or 4-chloronitrobenzene (Ding et al., 2013) and UV photochemical degradation of TCS produced photolysis products containing 1 or 2 chloride (dichlorohydroxydiphenyl ether, 2,4-dichlorophenol, monochlorohydroxydiphenyl ether, or monochlorophenol) (Sanchez-Prado et al., 2006). The differences between TCS and TCC in terms of structure and previously reported photodegradation products likely contribute to the difference in dechlorination efficacy for these two compounds.

As T-ZnO outperformed C-ZnO in dechlorinating TCS and TCC, additional time-course TCS and TCC photocatalytic experiments in the presence or absence of T-ZnO were conducted. In the absence of T-ZnO(i.e., control 2), there was 26% removal of TCS within 24 h under UV light (Fig. 2a). In the presence of T-ZnO, enhanced TCS removal was observed; i.e. approximately 95% of initial TCS (5 mg/L) within 12 h, followed by complete removal after 24 h of UV irradiation. The dechlorination efficiency of TCS increased continuously to reach approximately 65% in the first 12 h of the reaction, and levelling off as TCS was almost degraded afterwards (Fig. 2b). The initial removal kinetic constant k was estimated to be 0.296 min^{-1} based on data observed before 6 h of UV exposure (Table 1). Overall, our results are consistent to previous findings that TCS can be removed completely within 6 h by TiO_2 under the UV light. The reaction time is shorter due to a stronger UV source (15 W) used versus this study (4 W), but data on dechlorination of TCS was not available in their study (Yu et al., 2006).

Removal and dechlorination efficiency of TCC were different from those observed from TCS. Removal of TCC within 48 h was low in the absence of UV light (control 1) or T-ZnO (control 2), i.e., 15% and 20% TCC, respectively (Fig. 2c). In the presence of T-ZnO, approximately 58% of the initial TCC was degraded within 48 h, with an initial degradation rate constant of 0.023 min^{-1} for TCC based on the first 12 h data (Table 1). During the first 12 h, the amount of chloride released from TCC dechlorination increased, accounting for 50% of total chloride recovery based on the amount of TCC degraded. Additional UV exposure resulted in more chloride release, reaching a complete chloride recovery based on the amount of TCC degraded over 48 h (Fig. 2d). A previous study has shown complete TCC removal using a strong UV source (Hg or Xe lamp, 300 W) for 10 min, while dechlorination of TCC was not determined in their study (Ding et al., 2013). The incomplete TCC removal observed in this study might be due to the low UV intensity. Nevertheless, such low UV intensity was sufficient to degrade TCS within 12 h.

3.3. Reusability of T-ZnO

The reusability of T-ZnO is a critical factor for practical applications to remove emerging contaminants in reclaimed water. In this study, dechlorination efficiency of antimicrobial agents (TCS and TCC) by T-ZnO was used to assess the reusability of T-ZnO. As shown in Fig. 3, TCS and TCC dechlorination efficiencies were similar for three repeated treatments, suggesting that T-ZnO can be reused for at least three cycles. Previous studies showed that a ZnO layer synthesized by electrolysis on Zn can be used up to 4th or 5th times for recycling, maintaining its photocatalytic activity to about 75% in methylene blue degradation (Akhmal Saadon et al., 2016). This result demonstrated that ZnO as a photocatalyst could be reused at least three times on the degradation of chemical compounds under the UV light.

3.4. Inactivation of E. coli-pUC19

As T-ZnO-assisted photocatalysis resulted in better dechlorination efficiency for TCS and TCC than those of C-ZnO-assisted photocatalysis (see Section 3.2), T-ZnO was then used in inactivation experiments of *E. coli*-pUC19 and photocatalytic experiments with plasmid (pUC19). In the presence of T-ZnO, *E. coli*-pUC19 was inactivated effectively up to 94% after 3 h of UV exposure and almost of *E. coli*-pUC19 were inactivated after 12 h of UV exposure (4 W, 365 nm) (Fig. 4). In the absence of UV and ZnO (control 1), no inactivation of *E. coli*-pUC19 was observed over 12 h of incubation. Interestingly, when cells were exposed to T-ZnO but not to UV exposure (control 2), approximately 15% of cell inactivation was observed after 3 h of incubation which increased to 34% after total 12 h incubation. The results strongly suggest that T-ZnO itself has a bactericidal effect on *E. coli*-pUC19. The bactericidal effect of ZnO has been previous observed (Sirelkhatim et al., 2015). In the absence of T-ZnO, inactivation of *E. coli*-pUC19 increased from 9% after 3 h of UV exposure at 365 nm (4 W), to 67% inactivation after 6 h of UV exposure and then reached 97% inactivation after 12 h of UV exposure (control 3). This observation is consistent with previous findings that direct ultraviolet A (UVA, 315–400 nm), ultraviolet B (UVB, 280–315 nm), or ultraviolet C (UVC, 100–280 nm) have negative effects on bacterial cells (Kim et al., 2013; Lin and Wang, 2001). Our results demonstrated that T-ZnO promotes rapid cell inactivation under UV than sole UV exposure. These results are also consistent to results of previous studies using TiO_2 as photocatalysts (Kim et al., 2013; Liu and Yang, 2003).

While cells were inactivated by T-ZnO and/or UV exposure for 12 h, the pUC19 plasmids in inactivated *E. coli* were not damaged, based on the results of gel electrophoresis (Fig. S2 in SI). While the low intensity of UV irrigation used in this study was enough to inactivate cells, it was not sufficient to cause any structural damage of plasmid in the inactivated cells, a necessary step to remove the potential risk of spreading ARG to non-ARB via uptaking undamaged ARG-containing plasmids released from the lysis of inactivated ARB into the environment.

3.5. Photocatalysis of plasmid (pUC19)

To investigate whether photocatalysis can cause damage of ARGs-carrying plasmids and the function of photocatalyzed plasmids in other microorganisms following plasmid uptake, tests using circular plasmid (pUC19) in the presence of T-ZnO and UV light were

conducted. It is hypothesized that a break on plasmid DNA strand will cause a circular plasmid into a linear plasmid, leading to failure of expression of the genes carried in plasmids. In our case, we examined changes of circular plasmids into linear forms using gel electrophoresis. This is based on the fact that a same-size circular plasmid moves faster than a linear one during gel electrophoresis. The potential of photocatalyzed plasmids to be incorporated by live microorganisms and the function of the incorporated plasmids in the cells were also assessed using *E. coli* competent cells as described in the materials and methods section.

As shown in Fig. 5a, over 24 h of incubation, only one band (with a size of 1.6 kb) was observed for control 1 (containing pUC19 incubated at the dark), control 2 (containing pUC19 and T-ZnO incubated at the dark), and control 3 (containing pUC19 with UV exposure). The same band size is the supercoiled circle forms of the plasmid, suggesting that there was no damage of the plasmids in all controls. The lack of damage of DNA plasmids in Control 3 might be due to the lower UV intensity used in this study.

For T-ZnO samples, circular plasmids started to linearize after 3 h of UV irradiation as indicated by the presence of two bands, a 2.7 kb band (linear plasmid) and a 1.6 kb band (supercoiled circular plasmid). The intensity of the 2.7 kb band increased and the intensity of the 1.6 kb band decreased as UV exposure time increased. The plasmid DNA backbone was broken completely after 24 h of UV exposure, as indicated by the presence of the 2.7 kb band only (Fig. 5a).

Experiments were conducted to determine the transformation efficiency of plasmid DNA before and after photocatalysis with T-ZnO. The results were shown in Fig. 5b as a logarithmic scale of transformation efficiency. In the first 12 h of UV irradiation in the presence of TZnO, little transformation efficiency of photocatalyzed plasmid DNA was observed, however, an exponential decrease of transformation efficiency was observed after 12 h to 48 h (Fig. 5b). This observation corresponding to the results of the band pattern of gel electrophoresis suggest that the decrease of plasmid transformation efficiency was due to the linearization of the plasmid pUC19. Other studies have reported decreased transformation efficiency of plasmid DNA into *E. coli* after UV irradiation treatment and suggested the decrease was due to several conformational changes of the plasmid including linearization or nicking (Dietrich et al., 2005; Jiang et al., 2007). Exposure to UV has been known to break DNA backbone and modify double-stranded DNA (Chang et al., 2017; Kim et al., 2013). In this study, the low UV intensity alone was not sufficient to damage the circular plasmid.

4. Discussion

4.1. Implication of ZnO-assisted photocatalysis for emerging contaminant mixtures

An important finding of this research is that ZnO enhanced photodegradation of a range of concerned chemical contaminants in treated wastewater under low UV exposure without any pH adjustment. Previous TiO_2-assisted photodegradation study reported complete 1,4-dioxane removed by TiO_2 (1.5 g/L) at pH 5.0 within 25 min with a first order degradation rate constant (k) of 0.4 min^{-1} using a Hg-vapor lamp (100 W) (Alvarez-Corena et al., 2016).

In our study, with C-ZnO, 1 g/L and low UV intensity (4 W/m^2) without pH adjustment, we observed complete 1,4-dioxane removal and a modestly higher *k* value for 1,4-dioxane (0.456 min^{-1}) than that previously reported (Alvarez-Corena et al., 2016).

As halogenated degradation products like chlorinated dioxin (Buth et al., 2010) or chlorinated anilines (Ding et al., 2013) are also potentially toxic, using removal of halogenated contaminants like THMs, TCS, and TCC alone without considering the degree of dehalogenation may be problematic in assessing the efficacy of a given treatment process. In fact, the dehalogenation extent based on the recovery of chloride and/or bromide should be included in assessing the treatment performance. Son et al. reported incomplete removal of TCS (82%) by TiO_2 under strong UV exposure (450 W) for 10 min (Son et al., 2009). TCS was completely removed by ZnO in this study and the *k* value was higher even under the low UV intensity (4 W/m^2). Herein we have shown that complete removal of TCS can be achieved under low UV energy intensity. However, another antimicrobial agent, TCC, was not completely removed by ZnO under UV irradiation despite the longer reaction time. It may be due to the low solubility of TCC in water, leading to slow kinetics and dissolution during photocatalysis. Complete degradation of TCC might be possible if a longer reaction time was used.

<100% chloride recovery when TCS was completely degraded after 12 h (Fig. 2b) may be due to formation of chlorinated products in the solution or sorption of products onto the surface of T-ZnO. About 35% of chloride ion might be present in the TCS photolysis products, and they might be sorbed on the surface of T-ZnO. Comparing the dechlorination of TCC and TCS, TCC might be fully dechlorinated if the reaction time is extended, because TCC released more free chloride after another 24 h. Our reusability study showed that T-ZnO exhibited an increased dechlorination of TCS and TCC following a 2nd and a 3rd reuse (Fig. 3), which might be due to the sorption of chlorinated products generated from the previous photocatalysis onto the surface of spent T-ZnO. However, we were unable to detect any sorption of TCS and its degradation products on the surface of fresh and/or spent T-ZnO using EDX, which in part might be due to detection limit of this analytical technique (data not shown). A better analytical method is thus needed to demonstrate this aspect in future studies. Overall, our results implied that ZnO-assisted photocatalysis is a promising technology to degrade mixtures of emerging chemical contaminants in the treated wastewater. Yet, future studies using ZnO-based photodegradation for degrading contaminant mixtures in reclaimed water are needed to determine effective exposure time under different UV intensities.

4.2. Inactivation of pathogen and damage of circular DNA plasmid by ZnO

UV irradiation is a common disinfection method to inactivate microorganisms (Xie et al., 2011); however, little is known about UV exposure time and intensity that is needed to cause damages on circular DNA plasmid in order to inactivate the function of the circular plasmids. A recent study demonstrated that ARGs could be degraded during UV disinfection treatment, indicating by a decreased transformation efficiency (Chang et al., 2017). Moreover, pathogens could be inactivated by UV disinfection, and decreased inactivation time could be achieved through TiO_2-photocatalytic oxidation to cause structural change in

circular DNA plasmids (Kim et al., 2013). Inactivation of several pathogens have been observed by ZnO-photocatalytic oxidation under the UV light (20 W/m^2) (Liu and Yang, 2003) and even under visible light(10.8 J/cm^2 blue light) (Yang et al., 2018). In this study, *E. coli* containing ARGs as a pathogen was photocatalytic inactivated by ZnO as like the previous studies (Kim et al., 2013) even under the lower intensity of UV light.

Mechanisms involved in UV and TiO_2-based photocatalysis of bacterial inactivation have been intensively investigated (Sirelkhatim et al., 2015). Reactive oxygen species (ROS) generated during UV exposure and/or TiO_2-based photocatalysis have been shown to target various components of a bacterium, including cell membrane and nucleic acid (Pigeot-Rémy et al., 2011). Cell membrane disruption of *E. coli* has been shown due to lipid peroxidation by ROS (Dalrymple et al., 2010). Under longer UV exposure with TiO_2 as a photocatalyst, total DNA concentration of *E. coli* was decreased, suggesting nucleic acid damage in*E. coli* (Kim et al., 2013). As ZnO behaves similarly to TiO_2 in assisting ROS production during photocatalysis, similar cell inactivation mechanisms during ZnO-assisted photocatalysis are thus expected. While no experiments were conducted to investigate cell inactivation mechanisms by ZnO, the rapid inactivation of cells observed in this study might be due to cell membrane disruption caused by lipid peroxidation by ROS.

The UV dose of 86.4 kJ/m^2 (based on 4 W/m^2 for 6 h) is required to effectively inactivate pathogens, based on the results of our study. Our UV dose is higher than that previously reported (51 kJ/m^2) using 2 g/L ZnO on 20 W/m^2 for 40 min (Liu and Yang, 2003). The difference might be due to that only 50% of ZnO dose (as photocatalysts) was used in our study. Based on our experimental data, instead of using low intensity UV lamp, if 200 W of UV light is applied to inactivate different pathogens, a much shorter exposure time, ranging from 5 to 8 min, would be sufficient when T-ZnO is also present. Also, as observed in this study, additional UV exposure (equivalent to a UV dose of 346 kJ/m^2, based on 4 W/m^2 for 24 h) is required to cause plasmid DNA damage. This UV dose is smaller than that that reported by Kim et al. (1152 kJ/m^2) in their study involving TiO_2 at UV exposure intensity of 160 W/m^2 for 120 min (Kim et al., 2013). It showed that if 200 W of UV light is applied to damage the plasmid inside *E. coli*, a much shorter exposure time, ranging from 96 to 100 min, would be sufficient when TZnO is also present.

In the event that undamaged plasmids are released from inactivated cells into the environment, there will be a risk of spreading ARGs into nearby active microorganisms via plasmid uptake. In this study, we also showed that circular plasmid DNA was damaged by ZnO-photocatalysis and the damaged plasmid DNA could not be uptaken by another *E. coli*, based on results of lower transformation efficiency of the damaged plasmid. As ARGs are commonly present in circular plasmids (Müller et al., 2016), ZnO photocatalysis can be an effective way to prevent spreading out ARGs. Unlike results reported previously (Chang et al., 2017), we did not observe damage of plasmid DNA by direct UV exposure, which in part, it might be due to the low intensity of UV used in this study. Our results suggest that ZnO can not only accelerate the cell inactivation but it can also assist in damaging double-stranded circular DNA under low UV intensity. Mostly, the ARGs inside the pathogen was not damaged even it was reacted with ZnO under UV. A combination of a stronger UV

irradiation and a longer exposure time is recommended to eliminate the risk of spreading of ARGs in the environment.

5. Conclusions

In this study, emerging microbial contaminants such as *E. coli* and circular plasmid DNA were photocatalytically damaged by ZnO. Emerging chemical contaminants including triclosan, triclocarban, 1,4-dioxane, and trihalomethanes, were also photocatalytically degraded by ZnO. In steady of using the removal of parent halogenated compounds, it is important to demonstrate the stoichiometric release of chloride or bromide following THMs, TCS, and TCC photodegradation. Especially, triclosan and 1,4-dioxane were removed completely within 24 h and 12 h by T-ZnO or C-ZnO, respectively. T-ZnO was more efficient than C-ZnO as a photocatalyst in the photocatalytic degradation of antimicrobial agents. ZnO can be reused for photocatalytic degradation at least three times because the dechlorination efficiency of antimicrobial agents was similar after ZnO reuse. Overall, our results suggested that ZnO-assisted low UV photocatalysis is a promising treatment alternative to polish treated wastewater to remove undesired chemical and microbial contaminants simultaneously.

Supplementary Material

Refer to Web version on PubMed Central for supplementary material.

Acknowledgment

We would like to acknowledge TAMU Materials Characterization Facility (MCF) for work done with the SEM/EDX.

References

Abada BSA, 2016 Degradation of Poly- and Per-fluoroalkyl Substances (PFASs) Using Photocatalyst Zinc Oxide Civil Engineering. Master of science. Texas A&M University.

Akhmal Saadon S, Sathishkumar P, Mohd Yusoff AR, Hakim Wirzal MD, Rahmalan MT, Nur H, 2016 Photocatalytic activity and reusability of ZnO layer synthesised by electrolysis, hydrogen peroxide and heat treatment. Environ. Technol 37, 1875–1882. [PubMed: 26732538]

Alvarez-Corena JR, Bergendahl JA, Hart FL, 2016 Advanced oxidation of five contaminants in water by UV/TiO_2: reaction kinetics and byproducts identification. J. Environ. Manag 181, 544–551.

Buth JM, Steen PO, Sueper C, Blumentritt D, Vikesland PJ, Arnold WA, Mcneill K, 2010 Dioxin photoproducts of triclosan and its chlorinated derivatives in sediment cores. Environ. Sci. Technol 44, 4545–4551. [PubMed: 20476764]

Chang PH, Juhrend B, Olson TM, Marrs CF, Wigginton KR, 2017 Degradation of extracellular antibiotic resistance genes with UV254 treatment. Environ. Sci. Technol 51, 6185–6192. [PubMed: 28475324]

Dalrymple OK, Stefanakos E, Trotz MA, Goswami DY, 2010 A review of the mechanisms and modeling of photocatalytic disinfection. Appl. Catal. B Environ 98, 27–38.

Dietrich GJ, Szpyrka A, Wojtczak M, Dobosz S, Goryczko K, Zakowski L, Ciereszko A, 2005 Effects of UV irradiation and hydrogen peroxide on DNA fragmentation, motility and fertilizing ability of rainbow trout (*Oncorhynchus mykiss*) spermatozoa. Theriogenology 64, 1809–1822. [PubMed: 15921734]

Ding SL, Wang XK, Jiang WQ, Meng X, Zhao RS, Wang C, Wang X, 2013 Photodegradation of the antimicrobial triclocarban in aqueous systems under ultraviolet radiation. Environ. Sci. Pollut. Res 20, 3195–3201.

Draper WM, Dhoot JS, Remoy JW, Kusum Perera S, 2000 Trace-level determination of 1,4-dioxane in water by isotopic dilution GC and GC–MS. Analyst 125, 1403–1408. [PubMed: 11002923]

Du Y, Lv XT, Wu QY, Zhang DY, Zhou YT, Peng L, Hu HY, 2017 Formation and control of disinfection byproducts and toxicity during reclaimed water chlorination: A review. J. Environ. Sci 58, 51–63.

Estevez E, Cabrera Mdel C, Molina-Diaz A, Robles-Molina J, Palacios-Diaz Mdel P, 2012 Screening of emerging contaminants and priority substances (2008/105/EC) in reclaimed water for irrigation and groundwater in a volcanic aquifer (Gran Canaria, Canary Islands, Spain). Sci. Total Environ 433, 538–546. [PubMed: 22858460]

FDA, 2016 Safety and Effectiveness of Consumer Antiseptics; Topical Antimicrobial Drug Products for Over-the-counter Human Use.

Gee RH, Charles A, Taylor N, Darbre PD, 2008 Oestrogenic and androgenic activity of triclosan in breast cancer cells. J. Appl. Toxicol 28, 78–91. [PubMed: 17992702]

Gilday LC, Robinson SW, Barendt TA, Langton MJ, Mullaney BR, Beer PD, 2015 Halogen bonding in supramolecular chemistry. Chem. Rev 115, 7118–7195. [PubMed: 26165273]

Halden RU, Paull DH, 2005 Co-occurrence of triclocarban and triclosan in U.S. water resources. Environ. Sci. Technol 39, 1420–1426. [PubMed: 15819193]

Halden RU, Lindeman AE, Aiello AE, Andrews D, Arnold WA, Fair P, Fuoco RE, Geer LA, Johnson PI, Lohmann R, McNeill K, Sacks VP, Schettler T, Weber R, Zoeller RT, Blum A, 2017 The Florence Statement on Triclosan and Triclocarban. Environ. Health Perspect 125, 064501. [PubMed: 28632490]

Hand S, Wang B, Chu KH, 2015 Biodegradation of 1,4-dioxane: effects of enzyme inducers and trichloroethylene. Sci. Total Environ 520, 154–159. [PubMed: 25813968]

Healy MG, Fenton O, Cormican M, Peyton DP, Ordsmith N, Kimber K, Morrison L, 2017 Antimicrobial compounds (triclosan and triclocarban) in sewage sludges, and their presence in runoff following land application. Ecotoxicol. Environ. Saf 142, 448–453. [PubMed: 28458228]

Hong PY, Al-Jassim N, Ansari MI, Mackie RI, 2013 Environmental and public health implications of water reuse: antibiotics, antibiotic resistant bacteria, and antibiotic resistance genes. Antibiotics 2, 367–399. [PubMed: 27029309]

Jiang Y, Ke C, Mieczkowski PA, Marszalek PE, 2007 Detecting ultraviolet damage in single DNA molecules by atomic force microscopy. Biophys. J 93, 1758–1767. [PubMed: 17483180]

Kim S, Ghafoor K, Lee J, Feng M, Hong J, Lee DU, Park J, 2013 Bacterial inactivation in water, DNA strand breaking, and membrane damage induced by ultraviolet-assisted titanium dioxide photocatalysis. Water Res. 47, 4403–4411. [PubMed: 23764591]

Lee DG, Zhao F, Rezenom YH, Russell DH, Chu KH, 2012 Biodegradation of triclosan by a wastewater microorganism. Water Res. 46, 4226–4234. [PubMed: 22673343]

Lee DG, Chu KH, 2013 Effects of growth substrate on triclosan biodegradation potential of oxygenase-expressing bacteria. Chemosphere 93 (9), 1904–1911. [PubMed: 23890965]

Lee KM, Lai CW, Ngai KS, Juan JC, 2016 Recent developments of zinc oxide based photocatalyst in water treatment technology: a review. Water Res. 88, 428–448. [PubMed: 26519627]

Lin K, Wang A, 2001 UV mutagenesis in *Escherichia coli* K-12: cell survival and mutation frequency of the chromosomal genes *lacZ*, *rpoB*, *ompF*, and *ampA*. J. Exp. Microbiol. Immunol 1, 32–46.

Liu HL, Yang TCK, 2003 Photocatalytic inactivation of *Escherichia coli* and *Lactobacillus helveticus* by ZnO and TiO_2 activated with ultraviolet light. Process Biochem. 39, 475–481.

Lv XT, Zhang X, Du Y, Wu QY, Lu Y, Hu HY, 2017 Solar light irradiation significantly reduced cytotoxicity and disinfection byproducts in chlorinated reclaimed water. Water Res. 125, 162–169. [PubMed: 28850886]

McMurry LM, Oethinger M, Levy SB, 1998 Triclosan targets lipid synthesis. Nature394, 531–532. [PubMed: 9707111]

Müller V, Rajer F, Frykholm K, Nyberg LK, Quaderi S, Fritzsche J, Kristiansson E, Ambjörnsson T, Sandegren L, Westerlund F, 2016 Direct identification of antibiotic resistance genes on single

plasmid molecules using CRISPR/Cas9 in combination with optical DNA mapping. Sci. Rep 6, 37938. [PubMed: 27905467]

Nezamzadeh-Ejhieh A, Khodabakhshi-Chermahini F, 2014 Incorporated ZnO onto nano clinoptilolite particles as the active centers in the photodegradation of phenylhydrazine. J. Ind. Eng. Chem 20, 695–704.

O'Loughlin TE, Martens S, Ren SR, McKay P, Banerjee S, 2017 Orthogonal wettability of hierarchically textured metal meshes as a means of separating water/oil emulsions. Adv. Eng. Mater 19, 1600808.

Oskoei V, Dehghani MH, Nazmara S, Heibati B, Asif M, Tyagi I, Agarwal S, Gupta VK, 2016 Removal of humic acid from aqueous solution using UV/ZnO nanophotocatalysis and adsorption. J. Mol. Liq 213, 374–380.

Pigeot-Rémy S, Simonet F, Errazuriz-Cerda E, Lazzaroni JC, Atlan D, Guillard C, 2011 Photocatalysis and disinfection of water: identification of potential bacterial targets. Appl. Catal. B Environ 104, 390–398.

Pruden A, Larsson DG, Amezquita A, Collignon P, Brandt KK, Graham DW, Lazorchak JM, Suzuki S, Silley P, Snape JR, Topp E, Zhang T, Zhu YG, 2013 Management options for reducing the release of antibiotics and antibiotic resistance genes to the environment. Environ. Health Perspect 121, 878–885. [PubMed: 23735422]

Richardson SD, Kimura SY, 2017 Emerging environmental contaminants: challenges facing our next generation and potential engineering solutions. Environ. Technol. Innov 8, 40–56.

Roh H, Subramanya N, Zhao F, Yu CP, Sandt J, Chu KH, 2009 Biodegradation potential of wastewater micropollutants by ammonia-oxidizing bacteria. Chemosphere 77, 1084–1089. [PubMed: 19772981]

Rosario K, Nilsson C, Lim YW, Ruan Y, Breitbart M, 2009 Metagenomic analysis of viruses in reclaimed water. Environ. Microbiol 11, 2806–2820. [PubMed: 19555373]

Rose JB, 2007 Water reclamation, reuse and public health. Water Sci. Technol 55, 275–282.

Rule KL, Ebbett VR, Vikesland PJ, 2005 Formation of chloroform and chlorinated organics by free-chlorine-mediated oxidation of triclosan. Environ. Sci. Technol 39, 3176–3185. [PubMed: 15926568]

Sanchez-Prado L, Llompart M, Lores M, Garcia-Jares C, Bayona JM, Cela R, 2006 Monitoring the photochemical degradation of triclosan in wastewater by UV light and sunlight using solid-phase microextraction. Chemosphere 65, 1338–1347. [PubMed: 16735047]

Schneider J, Matsuoka M, Takeuchi M, Zhang J, Horiuchi Y, Anpo M, Bahnemann DW, 2014 Understanding TiO_2 photocatalysis: mechanisms and materials. Chem. Rev 114, 9919–9986. [PubMed: 25234429]

Sirelkhatim A, Mahmud S, Seeni A, Kaus NHM, Ann LC, Bakhori SKM, Hasan H, Mohamad D, 2015 Review on zinc oxide nanoparticles: Antibacterial activity and toxicity mechanism. Nano-Micro Lett. 7, 219–242.

Son HS, Ko G, Zoh KD, 2009 Kinetics and mechanism of photolysis and TiO_2 photocatalysis of triclosan. J. Hazard. Mater 166, 954–960. [PubMed: 19136205]

State Water Resources Control Board, 2018 Monitoring Strategies for Constituents of Emerging Concern (CECs) in Recycled Water, California.

USEPA, 2008 Reregistration Eligibility Decision (RED) Document for Triclosan.

USEPA, 2012 Guidelines for Water Reuse.

USEPA, 2017 Technical Fact Sheet — 1,4-Dioxane.

Wang FH, Qiao M, Lv ZE, Guo GX, Jia Y, Su YH, Zhu YG, 2014 Impact of reclaimed water irrigation on antibiotic resistance in public parks, Beijing, China. Environ. Pollut 184, 247–253. [PubMed: 24071635]

Xie Y, He Y, Irwin PL, Jin T, Shi X, 2011 Antibacterial activity and mechanism of action of zinc oxide nanoparticles against *Campylobacter jejuni*. Appl. Environ. Microbiol 77, 2325–2331. [PubMed: 21296935]

Yang MY, Chang KC, Chen LY, Wang PC, Chou CC, Wu ZB, Hu A, 2018 Blue light irradiation triggers the antimicrobial potential of ZnO nanoparticles on drug-resistant *Acinetobacter baumannii*. J. Photochem. Photobiol. B Biol 180, 235–242.

Yu JC, Kwong TY, Luo Q, Cai Z, 2006 Photocatalytic oxidation of triclosan.Chemosphere 65, 390–399. [PubMed: 16571361]

Zhu X, Yuan C, Bao Y, Yang J, Wu Y, 2005 Photocatalytic degradation of pesticide pyridaben on TiO_2 particles. J. Mol. Catal. A Chem 229, 95–105.

HIGHLIGHTS

- ZnO-assisted photocatalysis of 1,4-dioxane and THMs was effective.
- Photocatalytic activity of ZnO remains unchanged after three times of reuse.
- ZnO facilitated rapid inactivation of *E. coli* under low UV irradiation.
- Damages of ARGs-containing plasmids were observed by photocatalysis with only ZnO.

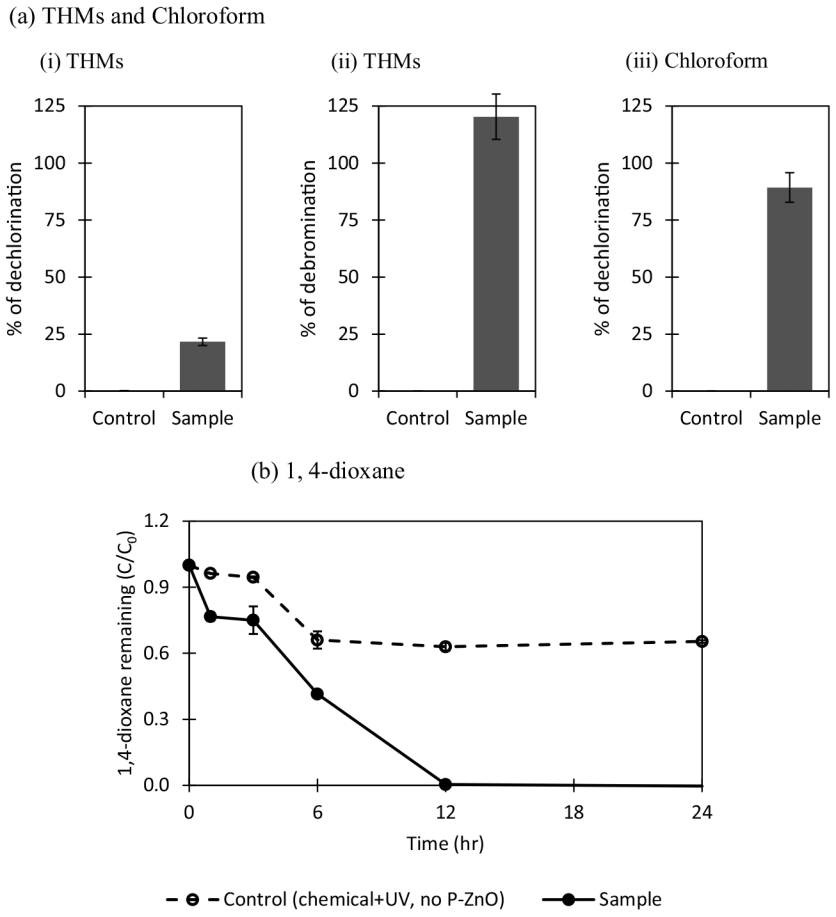

Fig. 1.

Photocatalysis of THMs, chloroform and 1,4-dioxane by C-ZnO. The experiments were conducted using 3 mg/L of THMs (or 3 mg/L of chloroform or 20 mg/L of 1,4-dioxane) and 1 g/L of C-ZnO at pH 7.0 with UV exposure (4 W, 365 nm) for 24 h. ZnO-free controls (i.e., chemical + UV) were used. (a) THMs and chloroform (i–ii) dechlorination and debromination was based on the theoretical amount of chloride or bromide ions that can be released from the amount of THMs photocatalyzed. One mol of THMs degradation = 6 mol of chloride (or bromine) released. For complete dechlorination of 3 mg/L THMs, 4.65 mg/L of free chloride and 6.8 mg/L of free bromide are expected to release into liquid medium. Overall dehalogenation efficiency is about 85%. (iii) Dechlorination of 1 mol of chloroform will release 3 mol of free chloride (i.e. 0.67 mg/L of free chloride release per 3 mg/L of chloroform degraded). (b) Removal of 1,4-dioxane. Each error bar is already shown in the figures.

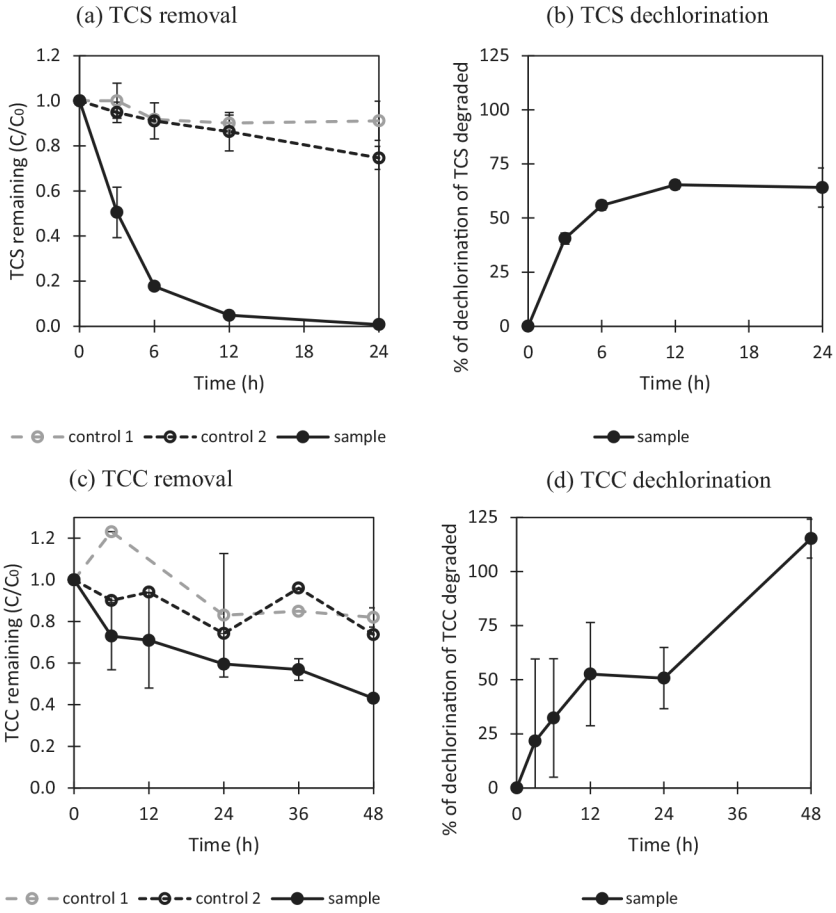

Fig. 2.

Photocatalytic degradation of antimicrobial agents. The experimental conditions were as follows: TCS or TCC 5 mg/L, ZnO 1 g/L, pH 7.0, UV light: 4 W, 365 nm, reaction time: 24 h or 48 h. Control 1: TCS or TCC and T-ZnO without exposure to UV light (TCS or TCC + T-ZnO + dark room), control 2: TCS or TCC with exposure to UV light (TCS or TCC + UV), sample: TCS or TCC and T-ZnO with exposure to UV light (TCS or TCC + T-ZnO + UV). (a) Photocatalytic removal of TCS. (b) Dechlorination of TCS: 3 mol of chloride should be theoretically released during 1 mol of triclosan degradation (1.84 mg/L of free chloride per 5 mg/L of triclosan). (c) Photocatalytic removal of TCC. (d) Dechlorination of TCC. 3 mol of chloride should be theoretically released during 1 mol of triclocarban degradation: 0.54 mg/L of free chloride per 1.6 mg/L of triclocarban which a degraded concentration during photocatalysis is. Each error bar is already shown in the figures.

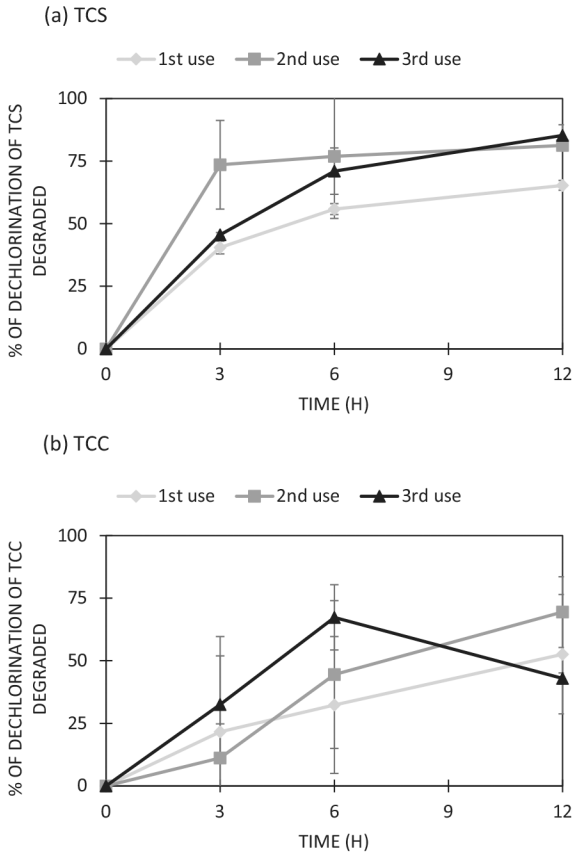

Fig. 3.

Reusability of T-ZnO for (a) TCS and (b) TCC photocatalysis. The experiments were conducted using 5 mg/L TCS (or TCC) and 1 g/L ZnO at pH 7.0 with UV exposure (4 W, 365 nm) for 12 h. The dechlorination rate was based on the theoretical amount of chloride that can be released from the amount of antimicrobial agent photocatalyzed. Each mole of TCS (or TCC) degraded is expected to release three moles of chloride in liquid medium. Each error bar is already shown in the figures.

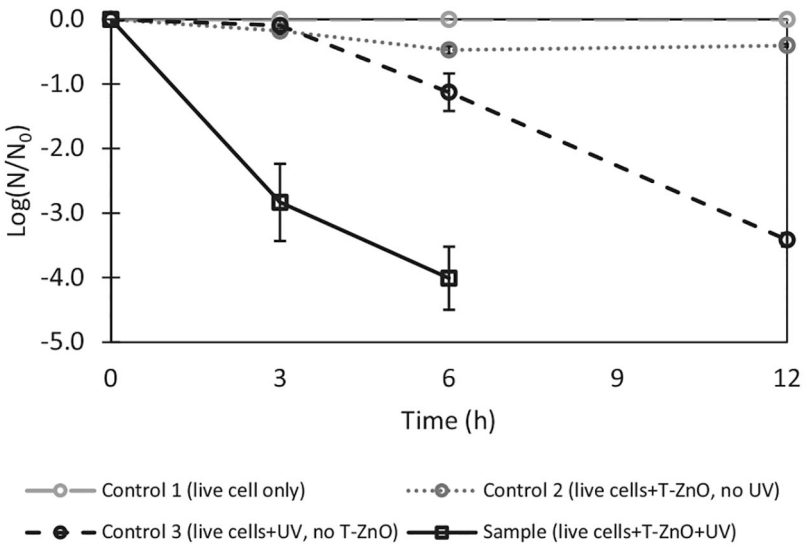

Fig. 4.

ZnO-assisted photocatalysis of *E. coli*-pUC19. The experiments were conducted using *E. coli*-pUC19 (optical density of 1.0) and 1 g/L of T-ZnO in 0.9% NaCl solution at pH 7.0 with UV exposure (4 W, 365 nm) for 12 h. The inactivation percentage of *E. coli*pUC19 is based on the numbers of colony forming unit (CFU) on the LB plates with ampicillin before and after UV treatment. Control 1 contains live cells without UV exposure (i.e., live cells only); control 2 contains live cells and T-ZnO without UV exposure(i.e., live cells + T-ZnO); control 3 contains live cells with UV exposure (i.e., live cells + UV). Sample contains live cells and T-ZnO with UV exposure (i.e., live cell + T-ZnO + UV). Each error bar is already shown in the figures.

(a)

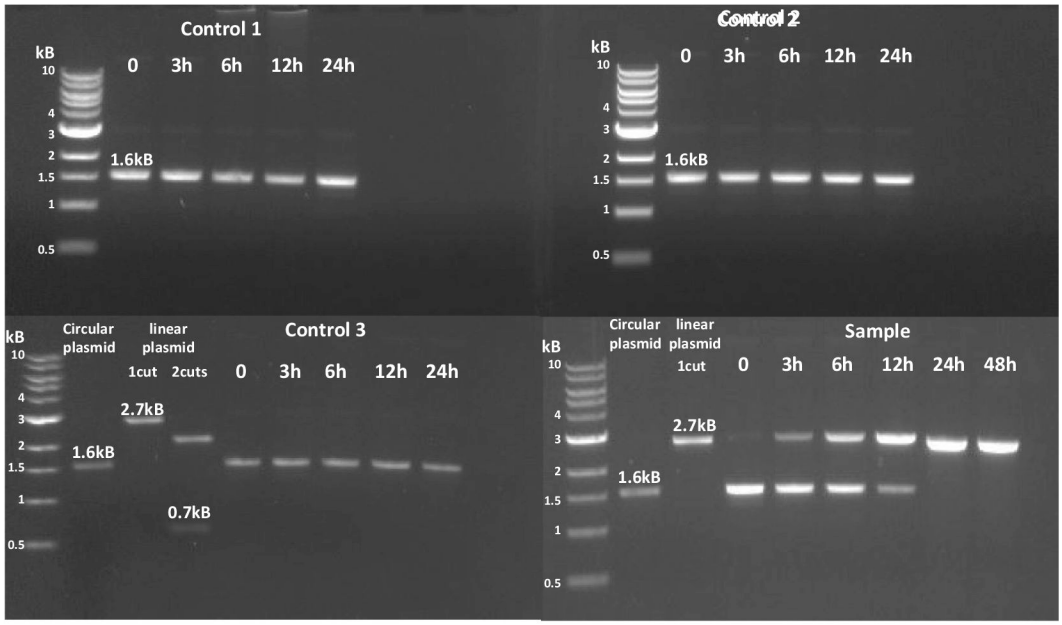

(b)

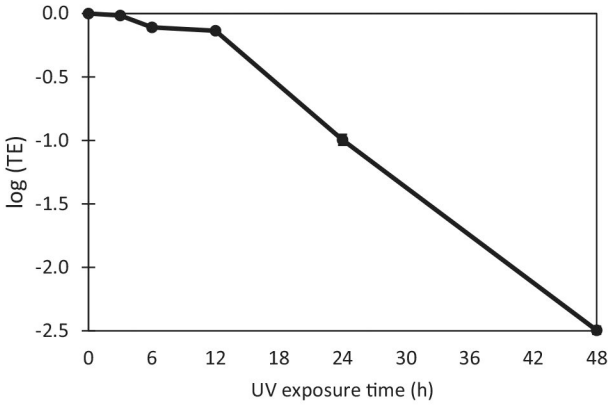

Fig. 5.

Effectiveness of T-ZnO and UV to cause damages on a circular plasmid (pUC19) that contains antibiotic resistance genes. Breaks in a circular plasmid DNA will cause change of a circular plasmid into a linear form (with one break), or multiple fragments (with multiple breaks). The total size of pUC19 is 2686 bp. Thus, an undamaged pUC19 (i.e., in its circular form) is expected to show on an electrophoresis gel with a band size smaller than 2.7 kb. When there is a break on the plasmid, the circular plasmid will become a linearized plasmid (i.e. 1 cut) and the size of band on an electrophoresis gel is expected to be around 2.7 kb. (a) Electrophoresis gel of plasmid DNA pUC19 showing breaks of pUC19 before and after photolysis by T-ZnO and/or UV exposure up to 48 h. Control 1 contains plasmid pUC19 without UV exposure (i.e., pUC19 only); control 2 contains plasmid pUC19 and T-ZnO without UV exposure(i.e., pUC19 + T-ZnO); control 3 contains plasmid pUC19 with UV exposure (i.e., pUC19 + UV). Sample contains plasmid pUC19 and T-ZnO with UV exposure (i.e., pUC19 + T-ZnO + UV). Circular plasmid Control without restriction enzyme,

linear plasmid for 1 cut with a restriction enzyme *Nde*I, 2 cuts with *Nde*I and *Pci*I were used. The expected sizes with 2 cuts are 2 kb and 0.7 kb. (b) The ability of treated plasmids to be uptake by other live microorganisms were estimated using competent *E. coli* with samples. It is shown as a log scale of transformation efficiency (TE). The TE of plasmids in the sample (i.e., pUC19 + T-ZnO + UV) is determined by counting the transformant CFU of each sample divided by transformant CFU of time zero samples. Each error bar is already shown in the figures.

Table 1

First order photodegradation rate constants for triclosan, triclocarban, and 1,4-dioxane under UV exposure in the presence and/or absence of ZnO. Data obtained before 6 h were used for estimating the constant for triclosan, while data obtained before 12 h were used for triclocarban and 1,4-dioxane.

Chemicals		First order degradation rate constant, k (min^{-1})
Triclosan (TCS)	UV	0.024 ± 0.006 (R^2 = 0.97)
	UV + T-ZnO (1 g/L)	0.296 ± 0.006 (R^2 = 0.99)
Triclocarban (TCC)	UV	0.005 ± 0.000 (R^2 = 0.35)
	UV + T-ZnO (1 g/L)	0.023 ± 0.000 (R^2 = 0.98)
1,4-Dioxane	UV	0.043 ± 0.003 (R^2 = 0.84)
	UV + C-ZnO (1 g/L)	0.456 ± 0.048 (R^2 = 0.88)